Physics Letters B 311 (1993) 317–323
North-Holland

PHYSICS LETTERS B

Diffractive W and Z production at $p\bar{p}$ colliders and the pomeron parton content

P. Bruni [a] and G. Ingelman [b,c]

[a] INFN, via Irnerio 46, I-40126 Bologna, Italy
[b] Deutsches Elektronen-Synchrotron DESY, Notkestraße 85, D-2000 Hamburg 52, FRG
[c] Department of Radiation Sciences, Uppsala University, Box 535, S-751 21 Uppsala, Sweden

Received 4 March 1993; revised manuscript received 8 May 1993
Editor: P.V. Landshoff

High-$p_\perp$ jets in diffractive $p\bar{p}$ events have revealed a parton structure in the exchanged pomeron. Based on a model using a pomeron structure function dominated by either quarks or gluons we calculate diffractive W/Z production and find observably large cross-sections at the Tevatron energy. The relative quark and gluon content may here be experimentally investigated and the x-shape of their density functions obtained to give new insights on the nature of the pomeron.

1. Introduction

Diffractive processes in hadron collisions [1] are well described, with respect to the overall cross-sections, by Regge theory in terms of the exchange of a pomeron ($\mathbb{P}$) with vacuum quantum numbers. In spite of this, the nature of the pomeron and its reaction mechanisms has remained a mystery, which was attacked in a new way [2] by considering hard scattering to resolve a possible quark or gluon content in the pomeron. Such a parton structure of the pomeron is natural in a modern QCD approach to the strongly interacting pomeron and it was, in fact, suggested long ago that the pomeron is mainly composed of gluons [3]. Thus, in the original model [2] for diffractive hard scattering the pomeron was assumed to behave essentially as a hadron and the concept of a pomeron structure function was introduced. By assuming such quark and gluon density distributions various hard scattering processes in pomeron–hadron and pomeron–lepton collisions have been calculated [2,4–7] and the resulting hadronic final states simulated [8,9].

The pomeron structure function need not be an a priori unknown quantity, but can be investigated theoretically. An analysis based on Regge theory has been made [4] and also an attempt to derive the pomeron gluon density distribution based on QCD ladder diagrams [10] giving a connection [6] to small-x physics in perturbative QCD. A large gluon content in a pomeron with small size would lead to large non-linear QCD effects from gluon recombination [11] that would be measurable at HERA [7].

In an alternative approach [12], the pomeron is argued to couple in an effectively pointlike way to single quarks (similar to a photon) and its effective structure function therefore dominated by a calculable quark–antiquark component (in analogy with the photon structure function).

On the experimental side the main result is the clear observation of diffractive hard scattering phenomena. The UA8 Collaboration at the CERN $p\bar{p}$ collider has indeed discovered [13] high-$p_\perp$ jets in diffractively produced high mass states, which signals hard parton level scattering in the pomeron–proton collision. The latest results [14] give evidence for a hard parton distribution in the pomeron, but cannot distinguish between a quark or gluon dominated pomeron. The evidence for diffractive production of bottom mesons reported by UA1 [15], which would receive a dominant contribution from the subprocess $gg \to b\bar{b}$, hints at a substantial gluon content with a soft momentum

0370-2693/93/$ 06.00

distribution in the pomeron but could hardly be explained by a quark-dominated pomeron [9]. It is obvious that more experimental information is needed in order to understand the quark/gluon composition of the pomeron. To this end we here consider W and Z production in single diffractive $p\bar{p}$ events at collider energies, which to leading order can only occur based on a quark component in the pomeron.

2. The model

The process we consider proceeds in two steps as illustrated in fig. 1. First, a pomeron is emitted from the (anti)proton at the upper vertex with a small squared momentum transfer, $t = (p_i - p_f)^2$, and with a fraction $x_{\mathbb{P}} = 1 - x_p \lesssim 0.1$ of the beam momentum p_i ($x_p = p_f/p_i$). In the second step this pomeron interacts with the proton in a large momentum transfer process between constituent partons. This pomeron factorisation [2,4], which may be justified by pomeron phenomenology for elastic and diffractive scattering [1], allows us to write the diffractive W, Z production cross-section as

$$\frac{\mathrm{d}\sigma(p\bar{p} \to \bar{p} + W/Z + X)}{\mathrm{d}x_{\mathbb{P}}\,\mathrm{d}t\,\mathrm{d}x_1\,\mathrm{d}x_2} = f_{\mathbb{P}/p}(x_{\mathbb{P}}, t)\frac{\mathrm{d}\sigma(\mathbb{P}p \to W/Z + X)}{\mathrm{d}x_1\,\mathrm{d}x_2}. \qquad (1)$$

The pomeron "flux" factor can be taken [2] as the ratio of the single diffractive cross-section and the pomeron–proton total cross-section,

$$f_{\mathbb{P}/p}(x_{\mathbb{P}}, t) = \frac{\mathrm{d}\sigma/\mathrm{d}x_{\mathbb{P}}\,\mathrm{d}t}{\sigma(\mathbb{P}p \to X)} = \frac{1}{x_{\mathbb{P}}}\left(6.38\ \mathrm{e}^{8t} + 0.424\ \mathrm{e}^{3t}\right)\frac{1}{2.3}, \qquad (2)$$

where the simple parametrisation is obtained by fitting [16] the numerator to single diffractive cross-section data and the denominator is taken as $\sigma(\mathbb{P}p \to X) = 2.3$ mb obtained from a Regge analysis [4] of data on elastic and single diffractive scattering. This flux factor includes a factor two to take into account that either p or $\bar{p}$ may be quasi-elastically scattered in the single diffractive process. It is, however, somewhat uncertain due to $\sigma(\mathbb{P}p \to X)$ which may well depend on the pomeron–proton CMS energy [17]. Although this flux factor has a different functional form compared to the one given in [12], they give about the same numerical value in the region of small t which dominates the cross-sections calculated below.

The hard scattering cross-section is assumed to be independent of t and is given by

$$\frac{\mathrm{d}\sigma(\mathbb{P}p \to W/Z + X)}{\mathrm{d}x_1\,\mathrm{d}x_2} = f_{q/\mathbb{P}}(x_1) f_{q/p}(x_2)\hat{\sigma}(q\bar{q} \to W/Z) = f_{g/\mathbb{P}}(x_1)\, f_{q/p}(x_2)\hat{\sigma}(gq \to q + W/Z). \qquad (3)$$

The densities f of quarks and gluons in the pomeron and the proton are evaluated at the corresponding momentum fractions x_1, x_2 and using the scale $Q^2 = m^2_{W/Z}$. The parton level cross-section $\hat{\sigma}$, given in [18], is for the case of quarks in the pomeron dominated by the leading order process $q\bar{q} \to W/Z$ (fig. 1a), whereas for gluons in the pomeron one is forced to the next-to-leading order (α_s) process $q\bar{q} \to q + W/Z$ (fig. 1b) which results in a smaller cross-section. (The symbol q is here used generically for quarks and antiquarks to cover all subprocesses.)

Whereas the parton momentum density distributions for the proton are known in the x-region of interest here (we use set 1 in [18]) the ones for the

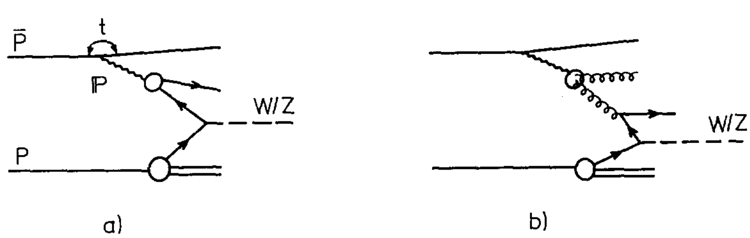

Fig. 1. Diffractive W/Z production in $p\bar{p}$ for a pomeron composed mainly of (a) quarks and (b) gluons.

pomeron are largely unknown and we illustrate this numerically by using the three alternatives

$$xf_{g/\mathbb{P}}(x) = 6(1-x)^5, \tag{4}$$

$$xf_{g/\mathbb{P}}(x) = 6x(1-x), \tag{5}$$

$$xf_{q/\mathbb{P}}(x) = \tfrac{6}{4}x(1-x). \tag{6}$$

Given this basic uncertainty we neglect any Q^2-evolution. The first two cases correspond to a pomeron dominated by many soft gluons ($\mathbb{P}$ = SG model) or a few hard ones ($\mathbb{P}$ = HG model), respectively. Although there are reasons to believe that the pomeron is a gluonic object [3] it could also contain a $q\bar{q}$ component. This can arise through QCD evolution from the gluons or be the main component as in the "pomeron–photon analogy" model [12]. Such a model can be represented, except for overall normalization, by our last case of a quark dominated pomeron ($\mathbb{P}$ = $q\bar{q}$ model). Whereas the first function has some support from the evidence for diffractive heavy flavour production [15], the latter two are more compatible with the observed diffractive jet production [14].

In all cases we have chosen the normalization such that the parton distributions fulfill the momentum sum rule

$$\int_0^1 \mathrm{d}x\, xf(x) = 1. \tag{7}$$

Although this is a natural expectation and can be given some motivation [4], it is by no means clear that this relation must hold for the pomeron which is a virtual exchanged object that need not behave as a normal hadron state. It does not hold for the pomeron model in ref. [12] where a smaller momentum integral results from its dominating quark density $xf_{q/\mathbb{P}}(x) \approx 0.2x(1-x)$, i.e. a factor 7.5 lower than in eq. (6). It is therefore important to keep in mind the uncertainty in this normalisation, but we note the possibility of adjusting it by a simple rescaling of the final results.

Using this formalism we have constructed a Monte Carlo program based on PYTHIA [19], exploiting its options to simulate W and Z production in hadron collisions. For the order α_s processes $q\bar{q} \to g + W/Z$ and $gq \to q + W/Z$ a cut $\hat{p}_\perp > 5$ GeV is applied on the parton level to avoid the usual divergences. The decay of the W/Z is properly treated as well as the remaining part of the event including initial and final state QCD parton showers and Lund model hadronization [19,20], resulting in a model simulating the complete interaction and final state.

3. Results

It is assumed in the following that the diffractive nature of the events can be ensured by detecting the quasi-elastically scattered (anti)proton or by imposing rapidity gaps. With a forward proton spectrometer, e.g. in roman pots, the values of the diffractive variables t and $x_{\mathbb{P}}$ can be determined. These are here integrated over the regions $|t| < 1\,\mathrm{GeV}^2$ and $x_{\mathbb{P}} < 0.1$.

Tables 1 and 2 give the cross-sections for both diffractive and non-diffractive W/Z production in $p\bar{p}$ collisions at $\sqrt{s} = 1.8$ (0.63) TeV corresponding to the Fermilab (CERN) collider. Since W and Z reconstruction from their hadronic decays is difficult, due to jet reconstruction and large background, we concentrate on the usually used leptonic decays $W \to \ell\nu_\ell$ and $Z \to \ell^+\ell^-$. Electrons and muons are here considered identifiable if they are within a typical detector acceptance of $|\eta| < 3$ and have $p_\perp^{e,\mu} > 20$ GeV to avoid large backgrounds from other sources such as heavy flavour decays. A neutrino is as usual infered from a large missing $p_\perp$. The symbol $\oplus$ in the tables refers to the sum of the corresponding processes/channels.

The tables demonstrate a stronger suppression of the diffractive cross-sections at the lower CMS energy as expected due to the relatively stronger effect of the W/Z mass threshold. The total diffractive W/Z cross-sections are therefore 20–40 times larger at the Tevatron energy and the observable lepton cross-sections up to factors of hundred larger depending on the pomeron model. These cross-sections should be considered in the context of the integrated luminosities, which at the Sp$\bar{\text{p}}$S is about 5 pb^{-1} in total per experiment and at the Tevatron one expects to collect some 100 pb^{-1} within the coming few years. For a quark-dominated pomeron the diffractive W/Z production can be up to about 3% of the total W/Z cross-section at the Sp$\bar{\text{p}}$S, which would imply the possibility to have collected a couple of Z's and some W's with

Table 1
Cross-section [pb] for Z^0 at $\sqrt{s}$ = 1.8 TeV ($\sqrt{s}$ = 630 GeV).

Model	Conditions	Parton level subprocess			
		$q\bar{q} \to Z^0$		$q\bar{q} \to gZ^0 \oplus gq \to qZ^0$	
non-diffractive	σ_{tot}	4400	(1300)	3000	(600)
	σ(observable $e^+e^- \oplus \mu^+\mu^-$)	230	(72)	150	(31)
$\mathbb{P} = q\bar{q}$	σ_{tot}	760	(32)	320	(8.4)
	σ(observable $e^+e^- \oplus \mu^+\mu^-$)	40	(1.6)	16	(0.3)
$\mathbb{P}$= HG	σ_{tot}	–	–	45	(1.4)
	σ(observable $e^+e^- \oplus \mu^+\mu^-$)	–	–	2.1	(0.02)
$\mathbb{P}$= SG	σ_{tot}	–	–	23	(0.54)
	σ(observable $e^+e^- \oplus \mu^+\mu^-$)	–	–	0.8	(0.001)

Table 2
Cross-section [pb] for $W^\pm$ at $\sqrt{s}$ = 1.8 TeV ($\sqrt{s}$ = 630 GeV).

Model	Conditions	Parton level subprocess			
		$q\bar{q} \to W^\pm$		$q\bar{q} \to gW^\pm \oplus gq \to qW^\pm$	
non-diffractive	σ_{tot}	14000	(4000)	9700	(1800)
	σ(observable $e^\pm \oplus \mu^\pm$)	2500	(680)	870	(150)
$\mathbb{P} = q\bar{q}$	σ_{tot}	2800	(190)	1100	(40)
	σ(observable $e^\pm \oplus \mu^\pm$)	470	(30)	110	(4)
$\mathbb{P}$= HG	σ_{tot}	–	–	180	(6)
	σ(observable $e^\pm \oplus \mu^\pm$)	–	–	28	(0.6)
$\mathbb{P}$= SG	σ_{tot}	–	–	100	(1.8)
	σ(observable $e^\pm \oplus \mu^\pm$)	–	–	12	(0.04)

leptonic decays in diffractive events if they passed the usual trigger conditions used for the W/Z analysis. On the other hand, a gluon dominated pomeron would never give more than about 0.1% diffractive W/Z's which would only give single W's. Thus, a search for W/Z events with a diffractive signature in existing data could give some information. The larger diffractive W/Z cross-section and the larger luminosity at the Tevatron leads to the expectation of many thousands of such events with observable leptonic decays in case of the $\mathbb{P} = q\bar{q}$ model used here and at least a thousand for the gluon model of the pomeron.

The $p_\perp$-distributions (figs. 2a, 2b) of muons from diffractively produced W/Z show the characteristic peak behaviour due to the boson mass. The cut $p_\perp >$ 20 GeV reduce the rates by 15–35% depending on the pomeron model. The muons are dominantly at rather central rapidities (figs. 2c, 2d) and should therefore largely be observable since the $p_\perp$-cut gives a reduction mainly at large rapidity, but only slightly in the central peak.

These differences in the rates of W/Z production in the different pomeron models should allow the possibility to distinguish between a pomeron dominated by quarks and gluons, respectively. It is, however, important to keep the above mentioned uncertainties in mind. Although variations of the pomeron flux factor would not change the relative rate of quark and gluon induced interactions, a better control of it would reduce the risk of misinterpreting a measured W/Z yield. With a proper theoretical framework the pomeron flux factor can be extracted from measurements of diffractive cross-sections at $p\bar{p}$ and ep colliders. The question of a saturated momentum

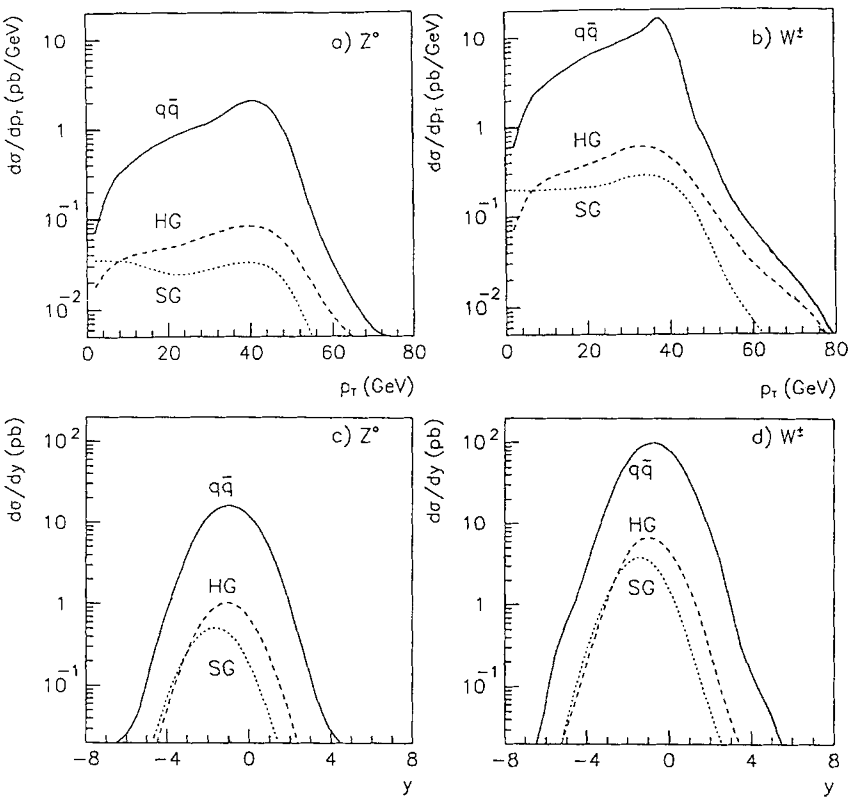

Fig. 2. Distributions of (a), (b) transverse momentum and (c), (d) pseudorapidity of muons from the decay of diffractively produced W/Z-bosons in $p\bar{p}$ collisions at $\sqrt{s} = 1.8$ TeV as obtained from different pomeron models: $\mathbb{P} = q\bar{q}$ (full), $\mathbb{P} =$ hard gluons (dashed), $\mathbb{P} =$ soft gluons (dotted).

sum rule applies to both the quark and gluon dominated pomeron structure function, but in case of non-saturation the rates need not be reduced by the same factor in the two cases. The difference between the quark and gluon induced W/Z cross-sections given above is, however, quite large such that a substantial difference remains even if only the quark structure function is reduced by the factor 7.5 discussed in connection with eq. (7). The quark/gluon content of the pomeron should therefore still be discernible and in any case be clearly revealed when the complementing information from diffractive production of jets and heavy flavours is taken into account.

Further information on the pomeron structure can be obtained through the possibility to reconstruct the x-shape of its parton distribution from the four-momenta of the W/Z decay leptons. Whereas electrons and muons are directly measured, the neutrino in W decay can only be obtained indirectly. Its transverse momentum is usually taken as the measured missing $p_\perp$ in the event and its longitudinal momentum can be obtained by the requirement $m_{\ell\nu_\ell} = m_W$ [21]. Since the accuracy of the resulting lepton momenta depends on details of the experimental apparatus, which is beyond the scope of our study, we have simply used the correct values in the following analysis. In the pomeron–proton collision, with CMS energy $\sqrt{s_{\mathbb{P}p}}$, one has for the process $q\bar{q} \to W/Z \to \ell\bar{\ell}$ the relations

$$\tau = x_1 x_2 = \frac{\hat{s}}{s_{\mathbb{P}p}} = \frac{(p_3 + p_4)^2}{s_{\mathbb{P}p}} = \frac{M^2_{W/Z}}{s_{\mathbb{P}p}}, \tag{8}$$

$$x_F = x_1 - x_2 = \frac{p_{3\parallel} + p_{4\parallel}}{\sqrt{s_{\mathbb{P}p}}/2}, \tag{9}$$

where p_3, p_4 are the four-momenta of the final leptons. Solving for the incoming parton momentum fractions

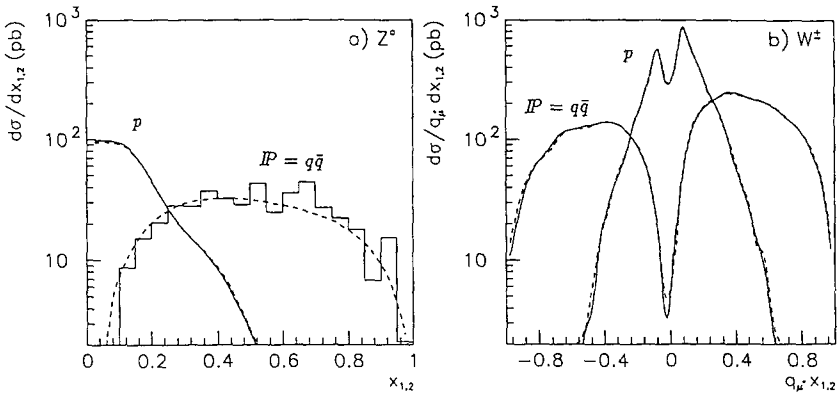

Fig. 3. Distributions of the momentum fractions x_1, x_2 for the interacting partons in the pomeron and proton, respectively. The curves/histogram correspond to the distributions used as input (dashed) and obtained through the reconstruction (full) from (a) $Z \to \mu^+\mu^-$ and (b) $W \to \mu\nu_\mu$ (q_μ is the muon/W charge); the histogram illustrates the statistical precision with $10\,\mathrm{pb}^{-1}$.

gives

$$x_{1,2} = \tfrac{1}{2}\left(\pm x_F + \sqrt{x_F^2 + 4\tau}\right). \tag{10}$$

Applying this method on the leptons, with $|\eta| < 3$ and $p_\perp > 20$ GeV, in our simulated events we obtain the measure shown in fig. 3 that directly reflects the pomeron and proton structure functions. In the W-case the charge of the lepton is included in the x-variable giving the asymmetry in fig. 3b due to the different hardness of the u- and d-quark distributions in the proton. There is a quite good agreement with the input distributions, which in the W-case will be less impressive when the experimental error on the neutrino reconstruction is taken into account. The illustrated statistical precision, which corresponds to 10 pb^{-1} and no acceptance/efficiency losses, shows the feasibility of this kind of measurement.

For the gluon-dominated pomeron this method is not appropriate due to the extra parton in the final state. Keeping only events where the extra parton has low energy (i.e. no extra jet) and therefore does not disturb the method may be possible, but will reduce the statistics. Alternatively, one could attempt to reconstruct the momentum of the extra parton (jet) and include it in the analysis to obtain less of a bias in the result. In any case, Monte Carlo studies can give an understanding of the bias such that useful conclusions on the x-shape can still be drawn.

4. Conclusions

The cross-sections for diffractive W/Z production at the Tevatron are expected to be large enough to give observable rates and the W/Z decay leptons to be mainly within the detector acceptance region so that the pomeron structure function can be reconstructed precisely enough to be of interest. This diffractive hard scattering process should be a useful tool in order to distinguish between a pomeron that is mainly composed of quarks or gluons. However, one has to keep in mind the uncertainties in the models for the pomeron, e.g. related to the pomeron flux factor and the question whether the pomeron structure function saturates the momentum sum rule. Although one cannot exclude a systematic difference between quarks and gluons from the latter, these uncertainties mainly affect the common overall normalization.

Our cross-sections are not likely to be underestimates, but may be overestimated by a limited factor. Although a smaller observed rate would give less precise measurements, it would still help to solve these theoretical uncertainties. The non-observation of this kind of events would give constraints on the pomeron models by setting an upper limit on the quark content in the pomeron and the normalization of its gluon content. The experimental measurements advocated here is therefore a "no-lose game" which, independent of the outcome, would give new insights on the nature of the pomeron.

References

[1] K. Goulianos, Phys. Rep. 101 (1983) 169.
[2] G. Ingelman and P. Schlein, Phys. Lett. B 152 (1985) 256.
[3] F.E. Low, Phys. Rev. D 12 (1975) 163;
S. Nussinov, Phys. Rev. Lett. 34 (1975) 1286; Phys. Rev. D 14 (1976) 246.
[4] E.L. Berger, J.C. Collins, D.E. Soper and G. Sterman, Nucl. Phys. B 286 (1987) 704.
[5] H. Fritzsch, K.H. Streng, Phys. Lett. B 164 (1985) 391;
N. Arteaga-Romero, P. Kessler and J. Silva, Mod. Phys. Lett. A 1 (1986) 211;
K.H. Streng, in: Proc. HERA Workshop (Hamburg, 1987), ed. R.D. Peccei, Vol. 1 (DESY, Hamburg, 1988) p. 365.
[6] G. Ingelman, Nucl. Phys. B (Proc. Suppl.) 18C (1990) 172.
[7] G. Ingelman and K. Prytz, DESY 92-177, Z. Phys. C, in press.
[8] P. Bruni, G. Ingelman, A. Solano, in: Proc. Physics at HERA, eds. W. Buchmüller and G. Ingelman, Vol. 1 (DESY, Hamburg, 1991) p. 363.
[9] P. Bruni and G. Ingelman, in: Proc. Workshop on Small-x and diffractive physics at the Tevatron (Fermilab, September 1992).
[10] J. Bartels and G. Ingelman, Phys. Lett. B 235 (1990) 175.
[11] G. Ingelman, K. Janson-Prytz, Phys. Lett. B 281 (1992) 325.
[12] A. Donnachie and P.V. Landshoff, Phys. Lett. B 191 (1987) 309; Nucl. Phys. B 303 (1988) 634.
[13] UA8 Collab., R. Bonino et al., Phys. Lett. B 211 (1988) 239.
[14] UA8 Collab., A. Brandt et al., Phys. Lett. B 297 (1992) 417.
[15] K. Eggert (UA1 Collab.), in: Proc. Elastic and diffractive scattering (1987), ed. K. Goulianos, (Editions Frontières, 1988) p. 1;
K. Wacker, in: Proc. 7th Topical Workshop on Proton–antiproton collider physics, eds. R. Raja et al. (World Scientific, 1988) p. 611.
[16] A. Brandt, private communication.
[17] P. Schlein, in: Proc. Workshop on Small-x and diffractive physics at the Tevatron (Fermilab, September 1992).
[18] E. Eichten, I. Hinchliffe, K. Lane and C. Quigg, Rev. Mod. Phys. 56 (1984) 579; 58 (1986) 1047.
[19] T. Sjöstrand, PYTHIA 5.6 and JETSET 7.3, CERN-TH.6488/92.
[20] B. Andersson, G. Gustafson, G. Ingelman and T. Sjöstrand, Phys. Rep. 97 (1983) 31.
[21] UA1 Collab., C. Albajar et al., Z. Phys. C 44 (1989) 15.